Energy-Harvesting Thermoelectric Sensing for Unobtrusive Water and Appliance Metering

Bradford Campbell, Branden Ghena, and Prabal Dutta
Electrical Engineering and Computer Science Department
University of Michigan
Ann Arbor, MI 48109
{bradjc, brghena, prabal}@umich.edu

Abstract

Fine-grained energy metering in homes and buildings provides a promising technique for addressing the unmaintainable energy consumption levels of worldwide buildings. Metering electricity, lighting, natural gas, HVAC, occupancy, and water on a per appliance or room basis can provide invaluable insight when trying to reduce a building's energy footprint. A myriad of sensor designs and systems collect data on particular building aspects, but are often hampered by installation difficulty or ongoing maintenance needs (like battery replacement). We address these common pitfalls for water and heat metering by developing a small, energy-harvesting sensor that meters using the same thermoelectric generator with which it powers itself. In short, the rate at which the harvester captures energy is proportional to the heat production of the monitored appliance or pipe and this relationship allows us to estimate energy use simply based on the sensor's ability to harvest. We prototype our sensor in a bracelet shaped form-factor that can attach to a shower head pipe, faucet, or appliance to provide local hot water or heat metering.

Categories and Subject Descriptors

B.4.m [**HARDWARE**]: Input/Output and Data Communications—*Miscellaneous*

General Terms

Design, Experimentation, Measurement, Performance

Keywords

Water-Sensing, Energy Metering, Wireless Sensing, Energy-Harvesting

ENSsys'14, November 6, 2014, Memphis, Tennessee, USA
ACM 978-1-4503-3189-0/14/11
http://dx.doi.org/10.1145/2675683.2675692

1 Introduction

Detailed energy metering in buildings allows homeowners, tenants, and building managers to understand usage patterns and provides a starting point for reducing consumption. Alongside electricity and natural gas, water, especially hot water, is an important resource to monitor within a building. Identifying this need, many previous projects aim to use wireless sensors to meter water consumption at the point-of-use [1, 3, 6, 7]. To do this, these sensors are placed in showers, under countertops, or in maintenance closets, and powering the sensors in these locations becomes a challenge. AC outlets are often not present and batteries are cumbersome to replace.

One potential source of energy is readily available to water metering sensors, however: the temperature differential between the water in the pipe being monitored and the ambient air. When a water event, such as a shower starting, occurs, the temperature of the pipe will change relative to the ambient surroundings. This temperature differential (hot or cold) can be harvested with a thermoelectric generator (TEG) to power a sensor node. TEGs utilize the Seebeck effect in order to produce a voltage from a thermal gradient. The power produced by this effect is proportional to the temperature differential, but is typically quite small when used with water in a building. Previous work demonstrated the feasibility of this harvesting technique, but found that not all use cases could continuously support sensor node operation [7].

We contribute Thermes, a new design point in TEG powered water and heat metering space. Thermes lessens the harvesting requirements of the TEG by observing that the mere ability to harvest from a temperature differential provides enough evidence to detect when hot or cold water is flowing. No additional sensors or periodic sampling are required. Data is reported by transmitting a packet when sufficient energy has been harvested to do so. The rate of transmission is proportional to the energy available in the pipe.

By attacking water metering this way, we are able to both simplify the hardware needed and reduce the size of the device. Because evidence of the water event is encoded in single packet transmissions, we don't require a battery or large storage capacitor to sustain networking or routing protocols. Simplicity in hardware design creates reduced energy requirements, allowing Thermes to continuously sense water usage across many use cases, even with small TEGs.

This style of sensing is akin to the Monjolo architecture [4] in which the sensor is the energy-harvester's ability to charge. Using this design for water metering with TEG devices has a key difference from the AC electricity metering application Monjolo was originally described with: saturation. That is, the temperature differential across the TEG device drops as heat transfers from one side to the other. This causes the harvesting rate to decline over time, even if the water state does not change and the pipe remains a constant temperature. With AC metering, a constant load was expected to support a constant harvesting rate. To adapt to this difference we add a processing step to the stream of received packets to estimate when the water event started and stopped.

Simplifying the sensing requirements to just the ability to harvest permits the sensor to be more versatile than just water metering. Any activity that causes a temperature differential to appear and then dissipate when the activity ends can be metered with our approach. In Section 5.5 we demonstrate this by metering three appliances: a stove, toaster oven, and radiator. In this way the same hardware can monitor multiple points of energy consumption, better addressing the original motivation.

We evaluate the viability of this metering approach by testing two different sizes of TEGs on a test setup over a range of common shower water temperatures. Further, we show that we can estimate the duration of the water event by analyzing the harvesting rate of the sensor. Finally, we explore possible improvement and future work for our system.

2 Related Work

Monjolo is a energy metering architecture in which an energy harvesting front-end intermittently powers a packet transmitting core [4]. On each wakeup, a single packet is transmitted, and a fixed quanta of energy is used. In this way, the rate of packet reception is proportional to the amount of energy harvested. While the original Monjolo paper focuses on induced magnetic fields, Thermes extends the principle to function with a thermal harvesting front-end, facing new challenges as a result.

Previous work by Rizzon et al. examines wireless sensor networks for environmental monitoring within a datacenter [8]. They show that it is possible to harvest excess heat generated by a processor in operation through a thermoelectric generator. Their research focuses on utilizing highly intermittent heat for energy rather than monitoring the more continuous heat source created by running water.

Several systems exist which wrap around a pipe and sense water flow events. Previous work by Martin introduced DoubleDip, which monitors temperature changes and pipe vibration via an accelerometer, and harvests thermal energy to recharge its battery [7]. The work demonstrates a real-world deployment across several locations and shows that hot water supplies can provide enough energy to indefinitely power a node. Sprav monitors temperature and sound, but does not harvest energy and relies solely on its battery [3]. Both Sprav and DoubleDip wirelessly transmit data to smartphones or other base stations. UpStream demonstrates a system that uses audio only to determine water flow, but could only be deployed for a single week due to battery usage [6].

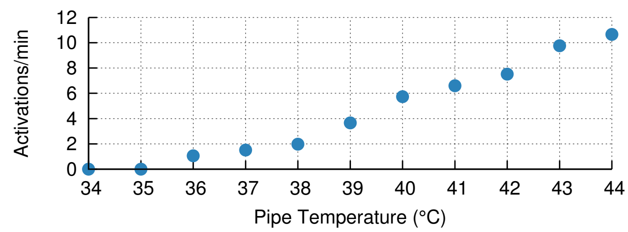

Figure 1: Activation rate of Thermes at a range of pipe temperatures in 23°C ambient conditions. As the temperature difference between each side of the Peltier module increases, so does the average rate of activations over the first five minutes of harvesting.

3 Design

Thermes is a true energy-harvesting water event detector based on the Monjolo principle of designing energy-harvesting sensors [4]. That is, if the desired phenomenon to be metered provides, directly or indirectly, a harvestable source of energy, then the simple act of harvesting provides insight into the desired phenomenon. We use a thermoelectric generator (TEG) and the temperature differential between hot water flowing in a pipe and the ambient air to harvest. The rate of harvesting is proportional to the temperature differential and, by extension, the temperature of the water in the pipe, as shown in Figure 1. To detect water events we note the rate at which the energy-harvesting power supply is able to harvest.

To achieve this, a power supply attached to the TEGs stores harvested energy in a bank of capacitors. Until the voltage of the capacitors reaches a certain level, the microcontroller and radio are power gated, allowing for a faster recharge rate than maintaining sleep mode. Once sufficient energy has been accumulated, the power supply activates the node which immediately transmits a packet. The node remains on until the stored energy reaches a lower threshold, ensuring that a fixed amount of energy is used on each activation.

Due to the operating regime of this sensing style and the small energy budget that accompanies it, the device itself knows little about what it is monitoring. Instead, an always-on central receiver service accepts the transmitted packets and processes them to understand properties of what is being sensed. The receiver calculates the rate of activations, or the rate of harvesting, based on the timestamp of the packets. Further, the service is responsible for estimating when the water event stopped and started. This is necessary both because there is a delay between when the pipe begins to heat and when the power supply is charged, and because the pipe will remain hot after the water stops causing additional activations.

The only state maintained on the microcontroller is an activation counter. This counter is transmitted in every packet and protects the system against dropped packets by allowing the receiver to calculate an average activation rate even if a packet is missed. Alternatively, this counter can be leveraged to rate-limit packet transmissions. For example, a transmission could occur every five activations, rather than on every activation.

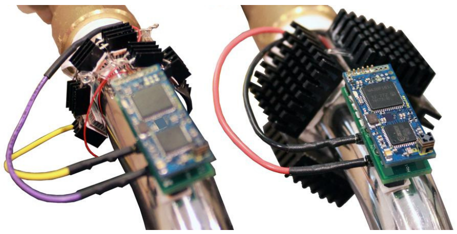

Figure 2: Thermes devices. On the left is the small bracelet of six 7 mm x 6 mm x 3 mm Peltier devices and nine 8.5 mm x 6 mm x 5 mm heatsinks. On the right is the large bracelet with four 15 mm x 15 mm x 3 mm Peltier devices and four 23 mm x 23 mm x 9 mm heatsinks. Both show the power supply and node core.

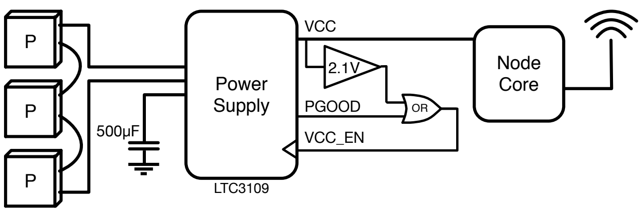

Figure 3: System Architecture. A series of Peltier devices provides a small input current to an LTC3109 based energy-harvester that charges a 500 µF bank of capacitors. The power supply enables the node core when the capacitor voltage reaches 3.1 V and leaves it enabled until the voltage drops below 2.1 V. The node core is responsible for counting its own activations and transmitting that count in a wireless packet.

This sensing style and design point allows for a small, wireless "bracelet" like device, composed of a series of TEG devices, the power supply, and a computation core, to be clipped around a pipe in order to monitor it. By not requiring a display, battery, or additional sensors, the size can be kept small for unobtrusive monitoring.

4 Implementation

To validate our design we built two prototype Thermes bracelets, as shown in Figure 2. The smaller and larger bracelets consist of heatsinks attached to six 7 mm x 6 mm and four 15 mm x 15 mm Peltier modules, respectively, a power supply board, and the computational core stacked on the power supply. The high-level design is shown in Figure 3.

4.1 Power Supply

The Thermes power supply is based on the Linear Technology LTC3109 [2] energy-harvesting IC. This IC is well suited for thermoelectric harvesting because of its low voltage requirement (30 mV) and auto-polarity feature which allows Thermes to be attached to hot or cold surfaces. The LTC3109 charges a 500 µF bank of capacitors and regulates its output to 3.3 V for running the microcontroller and radio.

The power supply disconnects its output V_{CC} rail when there is insufficient energy stored in the capacitors. This causes the microcontroller and radio to cold-boot on every activation. To trigger an activation we use the "power good" (P_{GOOD}) signal from the LTC3109 to enable V_{CC}. This P_{GOOD} signal triggers when the storage capacitors reach 3.1 V and

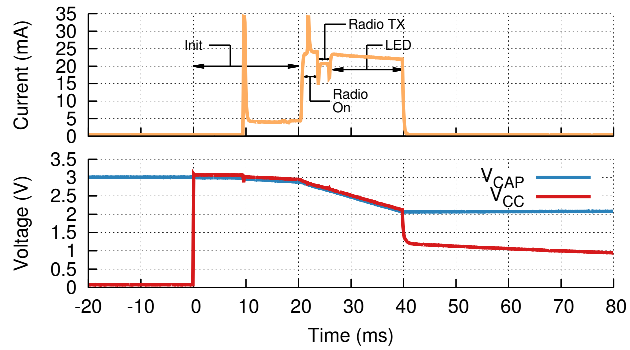

Figure 4: V_{CAP}, V_{CC}, and node core current draw during an activation. The current trace is annotated with the states of Thermes operation. When V_{CAP} reaches 2.1 V, V_{CC} is disabled and the node enters shutdown mode.

we use a latch circuit to keep V_{CC} activated until the capacitors drop to 2.1 V. This affords the microcontroller and radio sufficient time to transmit a packet (approximately 26 ms).

The power supply on the larger bracelet is fed by four CUI CP60133 Peltier modules wired in series and each attached to a heatsink. The smaller bracelet consists of six Laird 430779-512 Peltier modules wired as two parallel sets of three, and nine correspondingly smaller heatsinks with six attached to the TEGs and the additional three connected thermally. This design is sufficient to activate at higher temperature differentials, but at lower values the heatsinks saturate and harvesting ceases. This is explained further in Section 5.2.

4.2 Node Core

The node core is responsible for maintaining the activation counter and transmitting a packet after cold-booting. We use the components from the Epic [5] platform, namely the MSP430F1611 and CC2420, as well as FRAM nonvolatile storage to maintain the counter.

Upon boot, the node increments the counter in the FRAM, prepares and transmits an 802.15.4 broadcast packet containing the counter, and optionally enables an LED for visual feedback. A trace of this operation is shown in Figure 4. By integrating the product of V_{CC} and current, we find that each activation requires approximately 1.27 mJ of energy. If needed, this could be reduced by disabling the LED and configuring the power supply to disable the node core at a higher voltage than 2.1 V.

4.3 Collection and Processing

Once the central data processing service receives packets from a Thermes sensor, it estimates the start and stop times of the water event. To estimate the start time, the service compares the activation rate of the first few packets against calibration data with the observation that faster activations correspond to a smaller first packet delay. To estimate the end of the water event, the service determines when the activation rate decreases from its steady-state level and uses the timestamp of the last steady-state packets as the stop time. Currently, the calibration data for this algorithm is collected manually. In Section 6.4 we note a possible technique for automating the process.

Figure 5: Test measurement setup. A pump, point-of-use hot water heater, shower head, and tub simulate a shower, allowing for small-scale experiments with controlled temperatures.

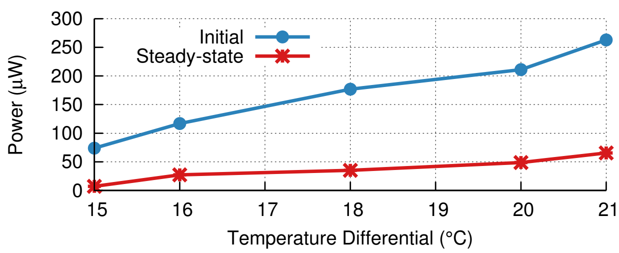

Figure 6: Power output of the power supply when using the large bracelet. The energy transferred to the storage capacitors is used to calculate the power output of the power supply over a range of initial temperature differentials at both startup (when the heatsinks are cool), and when the the saturation of the heatsinks reaches a steady-state.

5 Evaluation

To evaluate the viability of our design we use the controlled shower test setup shown in Figure 5. This allows for a constant water temperature and repeatable experiments.

5.1 Harvesting Power

First, we examine the power the larger bracelet and power supply can provide when exposed to temperature differentials between the water temperature and ambient air ranging from 15°C to 21°C. This was calculated by measuring the average rate of change in voltage of the 500 μF capacitor bank and incorporates all losses of heat transfer from the pipe to the Peltier module, the inefficiency of the Peltier module, and the inefficiencies in the power supply. As shown in Figure 6, the power generated by the power supply is much greater (averaging 4.3 times greater) when the water event first occurs than when the heatsinks reach a steady-state temperature. The low output power, peaking with the hottest water temperature at just 263 μW, is lower than expected based on the temperature and TEGs used. In steady-state, the average power output of the power supply was just 36.7 μW. While we show in Section 5.2 that our system can function on this anemic output, we expected better harvesting performance from the device. Some of this shortfall we contribute to our mechanical design, which we elaborate about in Section 6.

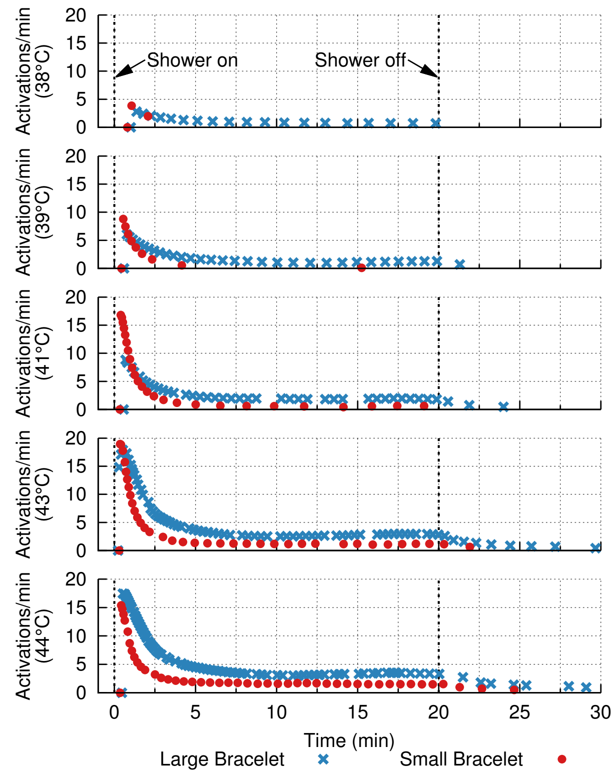

Figure 7: Activation rates of both bracelets for a 20 minute shower at different starting water temperatures and 23°C ambient conditions. Each mark on the graph denotes a received packet. The first packet is assigned a rate of zero. Gaps in packet receptions are likely due to dropped packets. At water temperatures below 41°C the small bracelet saturates quickly and is unable to regularly send packets over the entire duration. At 41°C and above, the pipe remains hot enough after water stops flowing to cause additional activations, however, the dropoff in rate signifies the end of the shower. Both bracelets demonstrate significantly higher activation rates initially than in steady-state, even though the water temperature is fixed. Overall, Thermes is able to harvest and transmit packets during the course of a shower at a range of common temperatures.

5.2 System Operation

To see how the intermittent Thermes device responds to a prolonged hot water event, we ran both bracelets attached to the shower arm for 20 minute simulated showers with water temperatures ranging from 38°C to 44°C. These temperatures encompass the range of common shower temperatures and a duration of 20 minutes was chosen to both be much longer than a typical shower and ensure that the harvester would reach steady state. The ambient air was constant at 23°C creating an initial temperature differential ranging from 15°C to 21°C. Figure 7 shows the results from the experiments. The vertical lines mark when the water event started and stopped. Each point on the chart denotes a packet reception and its y-value is the instantaneous activation rate calculated after receiving that packet.

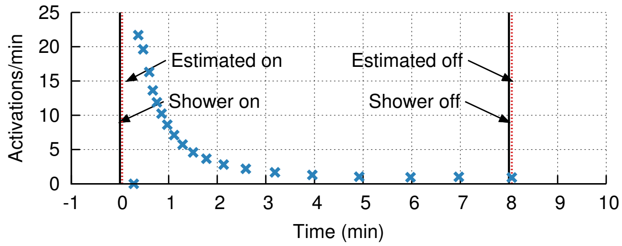

Figure 8: Water event monitored by Thermes with actual and estimated start and stop times. The actual water on and off times are indicated with solid black lines. The estimated times are based on received packets and calculate a water event duration that is 6 s longer than actual. While this is only one trial, the minimal error suggests that estimating duration based on received packets is a viable solution.

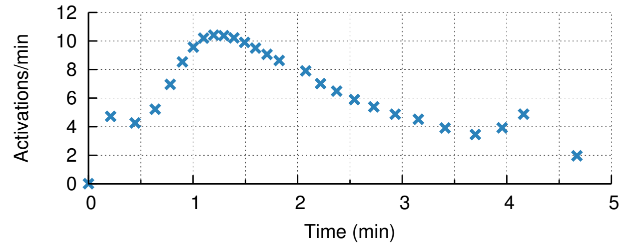

Figure 9: Activation rate of the smaller bracelet on an actual shower. The water was started briefly before the first packet arrived and ran for about twelve minutes. The initial dip and rise occur as the shower heats up. Packets stop before the five minute mark when the bracelet is unable to harvest.

First, we note the delay between when the shower began and when Thermes was able to successfully harvest and transmit a packet. For the small bracelet this delay ranged from 17.9 s to 48.1 s and averaged 26.7 s, and for the larger bracelet the delay ranged from 13.4 s to 60.3 s with an average of 34.4 s. Several factors can affect startup delay including residual heat in the pipe or heatsinks, residual charge in the capacitor bank, and water temperature. This delay causes error when calculating the exact duration of the water event, but can be partially compensated for by noting that larger temperature differentials have both a faster immediate response and a higher rate of initial activations. Therefore, the delay between water event start and first received packet can be estimated as a function of initial activation rate. An alternative way to address this issue is discussed in Section 6.4.

Second, we observe the effect of heatsink saturation at lower water temperatures. Below 41°C, the smaller bracelet and heatsinks are unable to maintain a temperature differential suitable for sustained harvesting. The larger heatsinks of the second bracelet, however, maintain a sufficient temperature differential over the entire time period. Further investigation is required to determine what size heatsink allows for continuous harvesting while optimizing overall device size.

Third, we notice that even though the water temperature remains constant, the activation rate of Thermes varies over time. For example, with 43°C water and the small bracelet, the activation rate varies between and 1.1 and 18.9 activations/minute at the extremes. This is in stark contrast to previous Monjolo designs, where saturation did not exist and a constant energy source implied a constant activation rate. This important difference is crucial to any future attempts to calibrate the devices or perform water metering.

Next, Thermes is susceptible to continued activations even after the water event ceases. Both bracelets transmit packets after the shower has stopped, particularly at the higher temperatures. This causes errors when detecting the total duration of the event. As before, activation rate provides a potential solution. When the water stops flowing, the activation rate of Thermes changes from a relatively constant steady-state to a noticeably slower rate. This sudden change can be detected and used to estimate when water likely stopped flowing.

Lastly, Figure 7 demonstrates the effects of dropped packets. While in steady state, the packets received should be evenly spaced; any gaps indicate a lost packet. The activation counter contained in each packet is meant to compensate for any drops and successfully reduces the effect of packet loss. This suggests that extremely low energy operation and a no-retry wireless MAC layer are acceptable for this application.

5.3 Post-Processing Events

To get a sense for how well Thermes is able to estimate the beginning and end of water events, we ran the smaller bracelet on the test setup with 42°C water. The plot of packets and activation frequencies is shown in Figure 8. The actual start and stop times of the shower are marked by solid black lines, and our estimates (using Section 4.3) are marked by dashed red lines. Based on the delays in other tests, we estimated that the first packet arrived 14 s after the start of the water event, resulting in an error of 3 s. Because we did not see a drop in activation rate we selected the end time as the last received packet, causing a 9 s error. The current algorithm only uses the time of an incoming packet as the end time, allowing up to one minute of error given the steady-state rate of this test.

5.4 Actual Shower

Figure 9 shows the result of using the small bracelet on an actual shower. The initial warm-up of the shower is recorded in the dip and rise of the activation rates. While the shower was about twelve minutes in duration, Thermes stops transmitting before five minutes have passed. Unlike on our test rig, the ambient temperature inside the bathroom increased while showering, negatively impacting Thermes's ability to harvest energy from the pipe. This further motivates the need for an improved mechanical design to better extract energy from the pipe and provide adequate heat dissipation.

5.5 Alternative Loads

Thermes's design allows it to be used to monitor other heat sources as well. As shown in Figure 10, it is possible to monitor an electric stove, toaster oven, or hot-water radiator. For the first two devices, we see the familiar curve, but with a slower rise to the peak activation rate as the attached surfaces heat more slowly. On the radiator, we see an immediate spike in activation rates because the radiator was already running when Thermes was attached. This mode is useful for appliances that are difficult to monitor by other means.

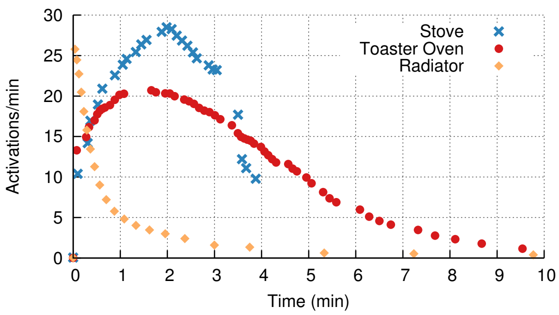

Figure 10: Operation when attached to a toaster oven, electric stove, and radiator. Thermes monitors three appliances that generate heat. By simply placing the bracelet on the oven or radiator pipe, or near the stove's heating coil, Thermes can detect when the appliances are used.

6 Discussion

In this section we address some potential issues and future work with the Thermes system.

6.1 Size

Size is an important factor of sensing devices installed at point-of-use. With four Peltier modules and their matching heatsinks necessary to support the expected measurement range, Thermes became larger than the non-obtrusive device we had hoped for. The cause of the size increase was the energy needs of our system. One option for improvement is to optimize the hardware and software to use less energy per activation by transmitting sooner.

Mechanical design also has a large role to play. As noted in DoubleDip [7], good thermal contact between the Peltier modules and the pipe is critical for performance. Current Thermes hardware relies on passive heat sink cooling. Better mechanical design of the heat sinks could both allow for more successful heat transfer to the air to prevent saturation of the device and reduce the size and count of Peltier modules.

6.2 Cost

When designing a system for indoor metering, the cost of metering must balance with the savings afforded by the data collection. One downside to thermoelectric harvesting with Peltier modules is their relative cost, particularly in smaller sizes (about 100 mm^2 and smaller). These devices range from one to 15 times the cost of a microcontroller. Therefore, scaling down in size while remaining within a reasonable cost range requires careful design and supply-chain planning.

6.3 Cooling and Temperature Effects

Thermoelectric harvesting depends on temperature differential, and maintaining this differential, particularly with a small device, becomes problematic. Heat sinks heat quickly when the monitored event is active, but cool slowly afterwards. This will cause successive events, such as back-to-back showers, to be troublesome. The second event may represent the same consumption of energy as the first but provide much less harvesting potential. Addressing this may require the central receiver to develop heuristics for determining when successive events did not provide enough cooling time and adjust its activation rate expectations.

6.4 Future Work

The Thermes design could be extended to better measure the magnitude of the metered heat source. By attaching a temperature sensor to the bracelet and sampling it at every activation, the receiver could better estimate the cost of water or heat events detected by different sensors. Further, this data could be used to build a calibration model for each sensor, allowing the activation rate to be directly converted to temperature and possibly energy.

7 Conclusions

Indoor point-of-use water monitoring sensors are essential for understanding resource and energy consumption pertaining to water in buildings. To aid deployability, these sensors have embraced energy-harvesting power supplies utilizing the temperature difference between pipes and ambient air. We exploit this observation by creating a water sensor that senses based entirely on its ability to harvest: if the device can power itself, then a water event must be occurring. This removes the need for external sensors or batteries, leading to smaller, and more deployable devices. We demonstrate the feasibility of this design point but note that scaling down in size requires further investigation into the mechanical design of the sensing device. Additionally, the generality of this sensing technique allows the same sensor to monitor other heat producing loads, furthering the energy monitoring capabilities of our design.

8 Acknowledgments

This work was supported in part by TerraSwarm, one of six centers of STARnet, a Semiconductor Research Corporation program sponsored by MARCO and DARPA. This material is based upon work supported by the National Science Foundation under grants CNS-1111541 and CNS-1350967, and the Graduate Research Fellowship Program under Grant No. DGE-1256260. This work partially supported by generous gifts from Intel and Texas Instruments.

9 References

[1] Amphiro. http://amphiro.com/.
[2] LTC3109 datasheet. http://cds.linear.com/docs/en/datasheet/3109fb.pdf.
[3] Sprav. http://www.sprav.com/.
[4] S. DeBruin, B. Campbell, and P. Dutta. Monjolo: An energy-harvesting energy meter architecture. In *Proceedings of the 11th ACM Conference on Embedded Networked Sensor Systems*, SenSys '13, 2013.
[5] P. Dutta, J. Taneja, J. Jeong, X. Jiang, and D. Culler. A building block approach to sensornet systems. In *SenSys'08: In Proceedings of the Sixth ACM Conference on Embedded Networked Sensor Systems*, Nov. 2008.
[6] S. Kuznetsov and E. Paulos. Upstream: motivating water conservation with low-cost water flow sensing and persuasive displays. In *Proceedings of the SIGCHI Conference on Human Factors in Computing Systems*. ACM, 2010.
[7] P. Martin, Z. Charbiwala, and M. Srivastava. DoubleDip: Leveraging thermoelectric harvesting for low power monitoring of sporadic water use. In *Proceedings of the 10th ACM Conference on Embedded Network Sensor Systems*, SenSys '12, pages 225–238, New York, NY, USA, 2012. ACM.
[8] L. Rizzon, M. Rossi, R. Passerone, and D. Brunelli. Wireless sensor networks for environmental monitoring powered by microprocessors heat dissipation. In *Proceedings of the 1st International Workshop on Energy Neutral Sensing Systems*. ACM, 2013.